

THE ACCURACY OF PRESENT MODELS OF THE HIGH ALTITUDE POLAR MAGNETOSPHERE

C. T. Russell¹, J. G. Luhmann² and F. R. Fenrich³

¹*Department of Earth and Space Sciences, University of California Los Angeles*

²*Space Sciences Laboratory, University of California Berkeley*

³*Department of Physics, University of Alberta, Canada*

ABSTRACT

The Polar satellite has explored the high-latitude, high-altitude magnetosphere out to 9 Earth radii (Re). The magnetic field data returned from this mission can be used both to provide data for new empirical models and to test existing models. Tests include comparing the observed location of the polar cusp with its position in the empirical models and comparing the strength of the magnetic field in the surrounding region. Near the cusp the magnetosphere is quite sensitive to solar wind conditions. In particular the energy density of the cusp plasma depends on the pressure of the solar wind applied to the interface of the cusp and the sheath. The applied pressure in turn depends on the shape of the magnetopause and the orientation of that interface, both controlled by the direction of the interplanetary magnetic field. Magnetohydrodynamic (MHD) models provide a coarse picture of the magnetosphere at high latitudes. While generally quite realistic, these too require testing against observations because even the MHD models must make some simplifying assumptions.

INTRODUCTION

Models embody our understanding of a physical system. There are many types of models, ranging from conceptual models of how processes work, to empirical models of the state of a system based on statistical studies of observational databases, to computer simulations of the physical processes governing the system. Each of these models has its particular strengths, limitations and ranges of applicability. The conceptual model is only as good as the understanding of the person who proposes the model and seldom is quantitative. An example conceptual model is the near-Earth neutral point model of substorms [Russell and McPherron, 1973]. An empirical, databased model is generally limited by the coverage of the observations. These limitations can be in the region surveyed, in the data types recorded or in the range of external conditions. An example of an empirical model is the Tsyganenko 96 model, one which used little high-latitude magnetic field data in its derivation, and covers only the magnetic field. Naturally it is based mainly on typical solar wind conditions and should not be expected to be very accurate for extreme solar wind conditions, for which there are few input data.

The third type of model is based on physical laws, and the usefulness and reality of the predictions of the model depend on the completeness of the physical processes included in the model. These models do not depend explicitly on satellites to have probed a particular region of space or for a particular solar wind condition to have occurred or have been observed. However, there is an implicit dependence through the testing of the models. A simple but elegant such model is the *Tsyganenko* [1989] magnetospheric magnetic field model based on the field of a dipole inside a superconducting ellipsoid of revolution. This model isolates the effects of the magnetopause currents for compressions of the magnetosphere by the solar wind and for changing tilts of the dipole. A more sophisticated model is the MHD simulation [e.g. *Fedder et al.*, 1997]. It contains much more physics (but not all). It computes a more complete set of plasma parameters, but it does so at a fairly coarse spatial resolution. Thus if the resolution of plasma boundaries is important this model may not be adequate.

A word should be said on the complementarity of spacecraft observations and computer simulations. Spacecraft provide a measurement at a particular point in space, but understanding the physics of the magnetosphere during the observation requires global context. At one time that global context was provided by magnetometer data and all sky camera data, but these have proven to be imperfect and subject to a variety of interpretations. The MHD simulation provides a global context based on solar wind input, and, if it can be verified with data near or at the key locations, the model can be used to gain much greater understanding than possible from the data alone.

In this paper we present information about the polar magnetosphere based mainly on the magnetic field observations that should be useful in developing and testing models. We compare data with some of the existing models and compare different types of models. This work is not exhaustive but rather illustrative of the behavior of the models.

THE POLAR MAGNETOPAUSE FOR NORTHWARD IMF

A key region for observations in the magnetosphere is near the reconnection site, whether that be on the magnetopause or in the current sheet in the tail. Because many missions have probed the low latitude magnetopause and because geometry controls the location of the reconnection site, it has been well probed for southward IMF. When the IMF is northward the magnetopause reconnection point moves to high latitudes above the poles and the geometry is not as well understood. A key objective of the Polar mission has been to provide a conceptual framework for this region as well as obtain the quantitative measurements that can be used in the next generation of empirical models.

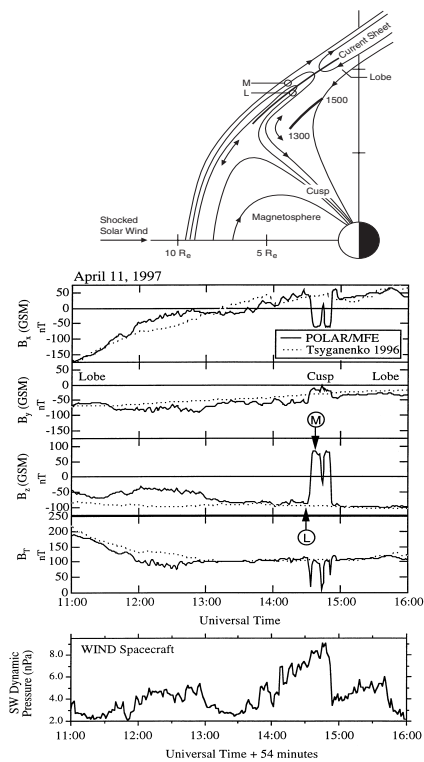


Fig. 1. Magnetic field measured by Polar and as predicted by the Tsyganenko 1996 model for the period 1100-1600 UT April 11, 1997, when the IMF was strongly northward. The top panel shows the location of Polar (solid line) for normal solar wind conditions. The points M and L appear to be on either side of the reconnection current layer (as sketched in the top panel) with Polar ‘moving’ in response to an increase in the solar wind pressure (shown in the bottom panel) [Russell et al., 2000].

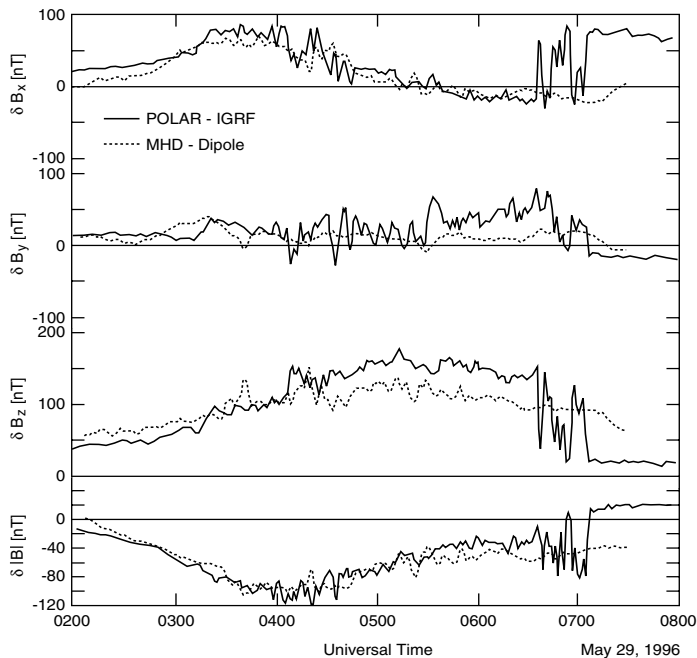


Fig. 2. Comparison of the magnetic field seen near the high latitude magnetopause on May 29, 1996 when the IMF was strongly northward. The solid line shows the magnetometer data and the dashed line the MHD simulation. The background field has been removed [Russell et al., 1998]. During this period the solar wind dynamic pressure was high and the IMF strongly northward. Polar remained close to the high latitude magnetopause, polar cusp and reconnection current layer this entire interval.

Recently some controversy has arisen on the nature of the magnetopause for strongly northward IMF [Fuselier *et al.*, 2000; Russell *et al.*, 2000] and whether parallel magnetic fields can reconnect. Figure 1 shows some of the data that have been at the center of this controversy. On April 11, 1997 the Polar spacecraft passed through the cusp and reconnection current sheet region coincident with an increase in the solar wind dynamic pressure shown in the bottom panel. The top panel shows a conceptual model of the magnetopause and reconnection site for the northward IMF conditions on this day. The line labeled 1300-1500 on these diagram shows where Polar would have been under normal solar wind conditions.

This diagram is important because it illustrates the complexity of this region and the incompatibility of our boundary region nomenclature developed at low latitudes. First the reconnection point is tailward of the region of the cusp at low altitudes. The field lines appear to have been pulled backwards toward the tail. In reality the plasma flow is away from the reconnection site so that if anything the field lines are moving toward the dayside at lower latitudes. The diagram shows a thin current layer across which the magnetic field reverses. This is the current sheet associated with reconnection. At low latitudes for southward IMF this current sheet is called the magnetopause. The name seems inappropriate here, since there is a second current layer further from the Earth across which the field switches to the direction of the draped magnetosheath field and the plasma becomes totally magnetosheath derived.

Since the field lines are shortening in this lower latitude region and being assimilated into the magnetosphere, the plasma flow must be away from the reconnection point. Thus the antisunward flow on these field lines that was present as they approached the magnetosphere has been stopped. There is a boundary where the magnetosheath flow is unaffected by the reconnection process. This region of velocity and magnetic field shear might more appropriately be called the magnetopause. In the interpretation of Russell *et al.* [2000], Polar effectively moved radially outward in this diagram in response to the increase in solar wind pressure cutting through the current sheet but not reaching the undisturbed solar wind flow.

This diagram also enables us to visualize where the polar cusp should be found relative to the magnetic field configuration. There are field lines that sweep back into the tail and those that bend back into the subsolar region. In other words there is a bifurcation in the magnetic field. For northward IMF the cusp plasma that has passed through the reconnection region heading toward the ionosphere is on the equatorward side of the bifurcation field line. For southward IMF it is on the poleward side. In undertaking studies with a magnetometer one may identify the bifurcation point near the magnetopause. Deeper in the magnetosphere the diamagnetic effect of the cusp plasma can be more clearly delineated and the bifurcation field line may not be identifiable.

A second period of strongly northward IMF with Polar near the magnetopause on May 29, 1996 has been even more thoroughly studied with multisatellite data [Savin *et al.*, 1998; Russell *et al.*, 1998], multi instruments [Scudder *et al.*, 2001] and MHD simulations [Russell *et al.*, 1998]. Figure 2 shows a comparison of the predictions of the MHD model based solely on the solar wind data with the magnetometer measurements on Polar. The background magnetic field (IGRF for Polar and a dipole for the simulation) have been removed from this plot. Overall there is very good agreement when Polar is in the closed field line region equatorward of the reconnection region but close to 0700 Polar approaches the reconnection point and crosses into the tail lobe. The MHD model does not predict this crossing. Part of the problem could be the coarseness of the simulation that does not produce current sheets as thin as observed. Also the strength of the magnetic field is predicted more accurately than the direction of the magnetic field as indicated by the components.

Despite these small discrepancies the MHD simulation serves a very useful purpose here because the comparisons shown in Figure 2 lend credence to the accuracy of the simulation and thus the simulations can be used to provide global context for the local observations. When the field lines of the model are traced to produce a diagram like that in Figure 1 a very similar pattern is seen.

THE LOCATION OF THE POLAR CUSP

The Polar spacecraft has provided much information on the location of the polar cusp as identified by the diamagnetic depression of the magnetic field strength. This signature has been compared with the plasma pressure simultaneously observed to confirm this identification. The location of the cusp depends principally on the

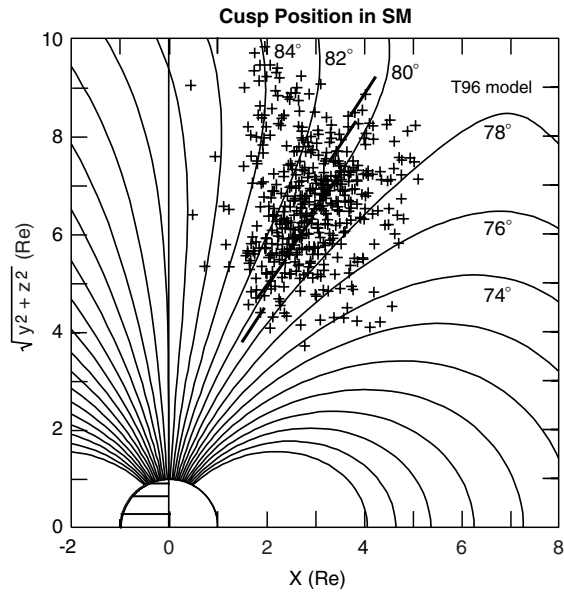


Fig. 3. Comparison of the location of the center of the cusp during individual cusp crossings by the Polar spacecraft plotted on magnetic fields in the noon-meridian derived from the Tsyganenko 96 model [Tsyganenko, 1996]. Here the dynamic pressure is taken to be 2 nPa, IMF $B_y=B_z=0$, and $Dst=0$.

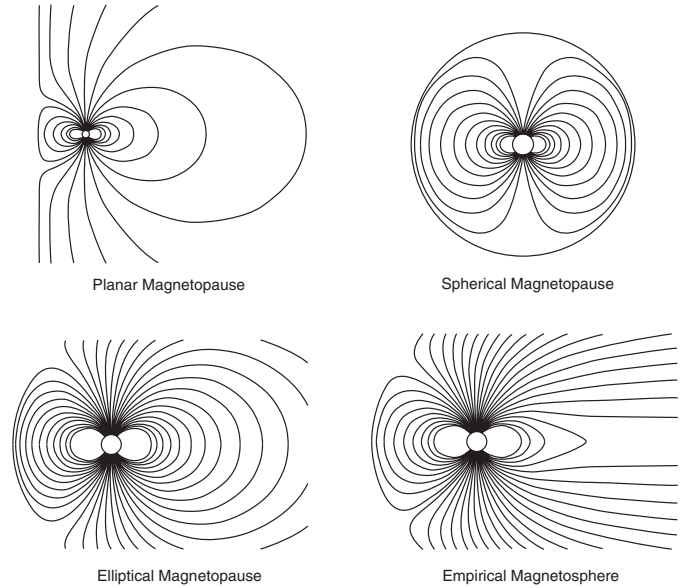


Fig. 4. Four magnetic field models with different shapes and plasma content illustrating the role of shape in controlling the magnetic field strength at the subsolar point. (Top left) Planar magnetopause causes a doubling of the subsolar field. (Top right) Spherical magnetosphere causes tripling of the subsolar field. (Lower left) Realistic ellipsoid of revolution comes an increase of a factor of 2.4. (Lower right) Empirical model mimics presence of plasma and proper shape and has factor of 2.4 increase of field at subsolar point.

direction of the IMF and the tilt of the dipole axis [Zhou *et al.*, 1999]. Figure 3 compares the locations of the polar cusp seen on Polar with a trace of the field lines in the T96 model. This compares two different quantities. The Tsyganenko model shows the location of the bifurcation of the magnetic field, and the polar cusp crossings show where the cusp plasma is. Nevertheless this display is useful because it illustrates that the cusp plasma is generally poleward of the T96 bifurcation point. Also this diagram implicitly shows that the complexity of the field seen near the cusp for northward IMF is not present in the T96 model.

SHAPE OF THE HIGH LATITUDE MAGNETOPAUSE

In order to develop a quantitatively correct model of the high latitude magnetosphere one needs to know the shape of the boundary. This is not simply because one needs to know where the boundary is but also because the solar wind pressure is applied to the magnetosphere along the normal to the magnetopause. Figure 4 illustrates this with four magnetospheric models. The top left model is the Chapman and Ferraro model with a planar magnetopause. At the subsolar point the magnetic field of the dipole is doubled just inside the boundary. In the spherical magnetosphere on the upper right the magnetic field is tripled in the equatorial region of the magnetopause. The bottom left diagram shows the elliptical magnetopause model of Tsyganenko [1989] that has a shape similar to that of the real magnetosphere. At the subsolar point the magnetic field is a factor of 2.4 greater than the dipole field.

As we move away from the subsolar point the pressure applied to the boundary drops as illustrated with Figure 5. There are three contributors to the pressure: the solar wind momentum flux, the interplanetary magnetic field and the static or thermal pressure. The solar wind dynamic pressure generally exceeds the magnetic and thermal pressure by a large factor, approximately the square of the appropriate Mach number. The magnetic pressure is anisotropic because no pressure is applied by a magnetic field along its length and the thermal pressure is anisotropic because there can be different pressures perpendicular and parallel to the magnetic field but we ignore these differences here. It is also worth noting that the solar wind is an inelastic fluid that flows around the

magnetosphere and does not bounce back elastically through the incoming flow. Thus the momentum flux is not doubled in calculating the dynamic pressure. The streamlines diverge as they approach the magnetopause further reducing the pressure in the surface by about 10%.

As illustrated in Figure 5 the normal stress of the solar wind on the boundary can be approximated with two terms one associated with the dynamic pressure, $\rho V^2 \cos^2 \alpha$, and one with the static and magnetic pressure, $P_{st} \sin^2 \alpha$ [Petrinec and Russell, 1997]. The former term is dominant in determining the standoff distance of the magnetopause, the strength of the magnetic field in the polar regions and the pressure of the plasma in the polar cusp. The latter term determines the asymptotic magnetic field strength in the tail and hence its radius. A key factor in predicting the correct field strength in the polar regions is to determine the correct shape of the boundary, i.e. the angle α , between the normal of the surface and the direction of the solar wind.

As might be expected most models of the dayside low latitude magnetopause under normal solar wind condition agree because there is much data at this location but away from the subsolar region and under atypical conditions the various models differ as shown in Figure 6 for the models of Petrinec and Russell [1993a] and Roelof and Sibeck [1993] for both high and low solar wind dynamic pressure. The standoff distance of the nose of the magnetopause varies with the B_z component of the interplanetary magnetic field as illustrated in Figure 7 [Petrinec and Russell, 1993b] but more recent studies suggest that the linear fit shown here is not applicable at the largest southward IMFs observed [Shue et al., 2001]. The flux that is eroded from the dayside magnetosphere is carried back into the magnetotail increasing its width and flaring angle with increasing southward IMF [Petrinec and Russell, 1993a].

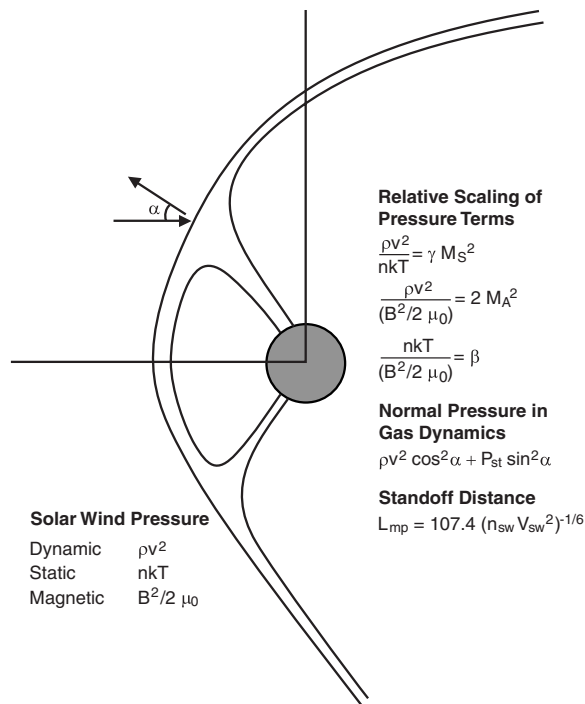


Fig. 5. The pressure applied to the magnetopause and polar cusp by the solar wind depends on the angle of the normal to the magnetopause and the solar wind flow velocity. The dynamic pressure far exceeds the static pressure over the dayside magnetopause, but beyond the terminator a correction for the static pressure becomes significant. Here M_A , M_s , β and γ use the Alfvén and sonic Mach numbers, the plasma beta and the polytropic index respectively. The expressions ρv^2 , nkT and $B^2/2\mu_0$ give the dynamic pressure, the static pressure and the magnetic pressure respectively.

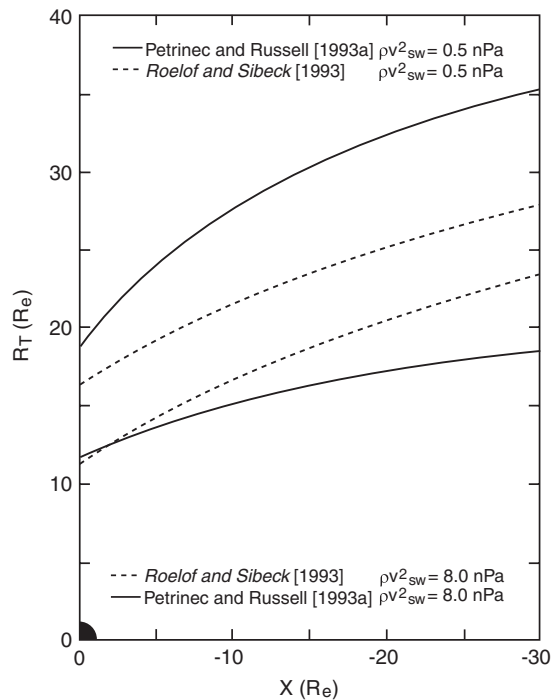


Fig. 6. Comparison of tail flaring for low and high-pressure solar wind conditions for the models of Petrinec and Russell [1993a] and Roelof and Sibeck [1993]. These two models give similar results for normal solar wind conditions but differ significantly for extreme conditions.

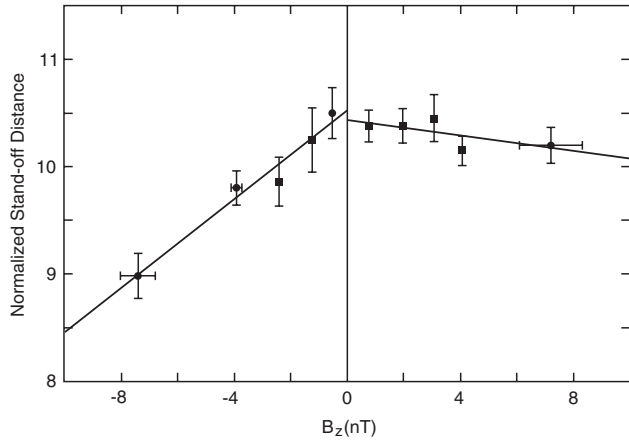


Fig. 7. The standoff distance of the nose of the magnetosphere as a function of IMF B_z [Petrinec and Russell, 1993a]. The straight lines are linear least square fits to the binned average magnetopause locations. The slope of the line for northward IMF is not significantly different than zero.

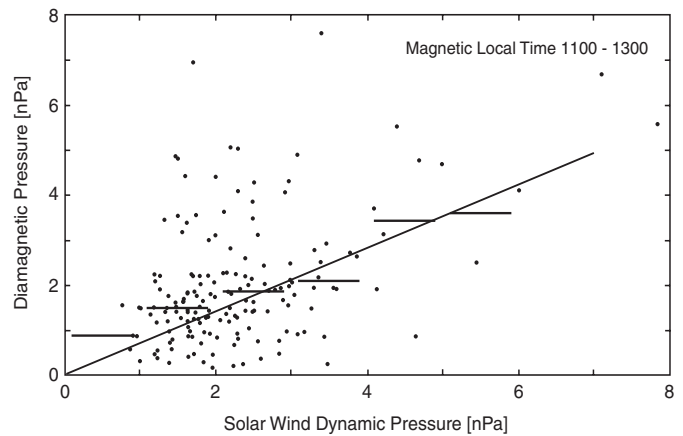


Fig. 8. Pressure of the plasma in the cusp versus the solar wind dynamic pressure in the noon sector. The bars give median pressures. The straight-line gives the theoretically expected value based on the shape of the cusp-magnetosheath interface [Zhou et al., 2001]. The agreement indicates that the shape of the magnetopause and cusp-magnetosheath interface are well known here.

THE EFFECTS OF PLASMA IN THE POLAR CUSP

If our paradigm of the polar cusp as being directly connected to the solar wind is correct, we can use our knowledge of the shape of the magnetopause to predict the pressure of the cusp plasma. We can measure the cusp plasma energy density by determining the depth of the drop in the magnetic energy density when the Polar spacecraft enters the polar cusp as determined from the low energy plasma measurements [Zhou et al., 1999]. This pressure is shown versus the simultaneous solar wind dynamic pressure in Figure 8. [Zhou et al., 2001]. The straight line on this figure is the expected variation based on the shape of the magnetopause determined near noon with the Hawkeye spacecraft [Zhou and Russell, 1997]. The predictions and the medians of the measurements agree quite well suggesting that the shape of the high-latitude magnetopause in the Zhou and Russell model is at least on average correct.

The data points in Figure 8 have been calculated as differences between the observed energy densities in the magnetic field inside and outside the cusp. Figure 9 shows the difference between the observed magnetic field and the T96 model during a cusp crossing on May 7, 1996 indicated by the rise in the electron and low energy ion density from 0500-0530 UT. As Figure 9 illustrates, the T96 model and the measured magnetic field do not agree in the region outside the cusp plasma, even though the observed pressure in the cusp plasma and the surrounding magnetic field can be shown to be in quantitative balance. The observed field is weaker than predicted and the energy density of the plasma in this region does not account for the difference in the magnetic pressure in the T96 model and the Polar observations. Figure 10 extends this case study by examining the difference in the predicted magnetic field as a function of dipole tilt and latitude. At both low latitudes and high the field strength is fairly accurately predicted, but around 60° the two differ greatly. Only part of this difference can be due to the pressure of plasma. We therefore conclude that the shape of the magnetopause, that controls the high latitude field strength in the T96 model, must differ from the actual magnetopause shape.

A COMPARISON OF THE T96 MODEL WITH MHD SIMULATIONS

Fenrich et al. [2001] have made detailed comparisons of the T96 empirical model with the Fedder and Lyons MHD code. As they point out the empirical model uses a magnetopause shape that has not been well observed at high latitude. In contrast while the magnetopause shape in the MHD code is self-consistent, viscosity and resistivity are arbitrary parameters. In T96 the plasma is implicit whether that plasma arises from the solar wind or the

ionosphere, while in the MHD code all the plasma is derived from the solar wind. There are no ionospheric sources in this MHD code. The T96 model has an adjustable ring current while there is no sensible ring current in the MHD model. The T96 model is always in an equilibrium state, while the MHD model allows one to follow the time history of dynamical processes. In both models the intrinsic resolution is coarse. Thin boundaries are not resolved in either model. In the T96 model interconnection with the IMF is imposed in an ad hoc manner. In the MHD model reconnection is controlled by the boundary conditions and physical processes. Also in the T96 model the distribution of field-aligned currents does not vary with the IMF although the strength does, while in the MHD model field-aligned currents are physically derived. In this section we illustrate the effects of these differences on the magnetic configuration of the magnetosphere with extracts from the Fenrich et al. paper.

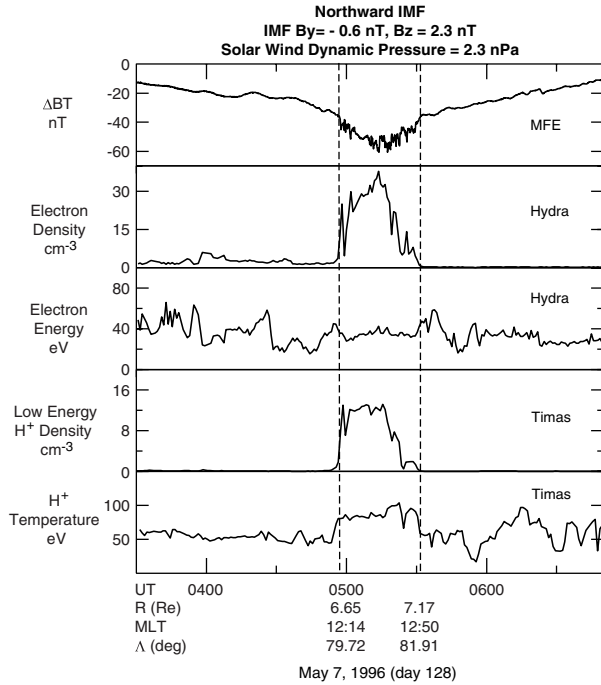


Fig. 9. Example of magnetic field and plasma signature in the polar cusp [Zhou et al., 2000]. The top trace shows the difference between the observed field and the predicted T96 field. The next two traces show the electron density and temperature from the Hydra instrument. The bottom two panels give a partial density and the corresponding proton temperature from the TIMAS instrument.

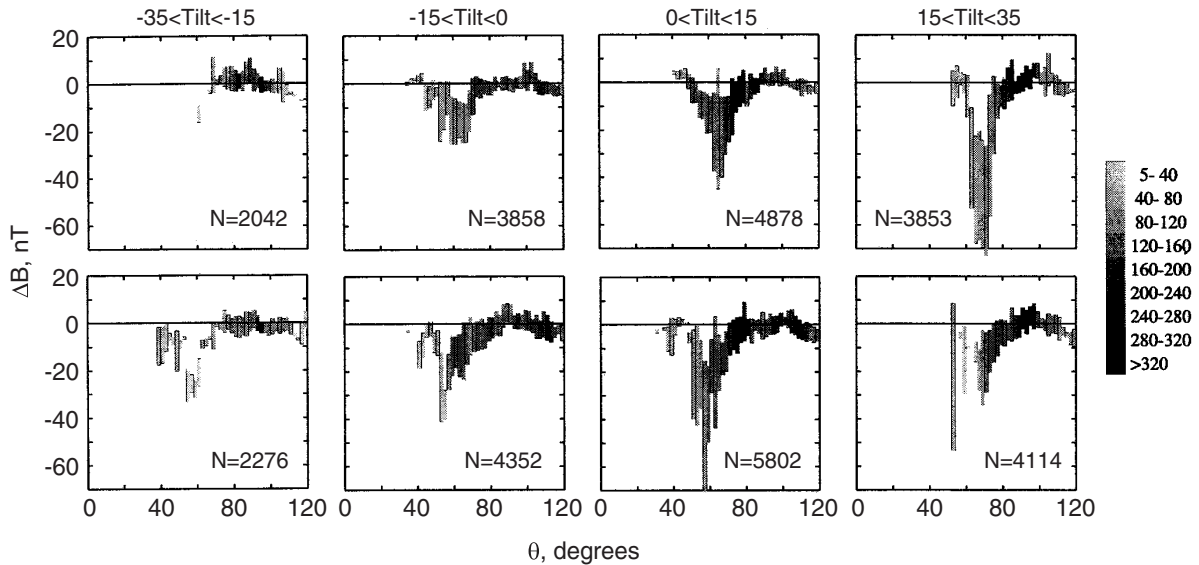


Fig. 10. Difference between the observed and T96 model magnetic fields as a function of solar magnetic latitude and tilt angle [Tsyganenko and Russell, 1999]. Top row shows statistics for northward IMF Bz and bottom row shows statistics for southward IMF Bz. Radial range is $7 \leq R < 8 R_E$. Gray scale indicates minutes of data.

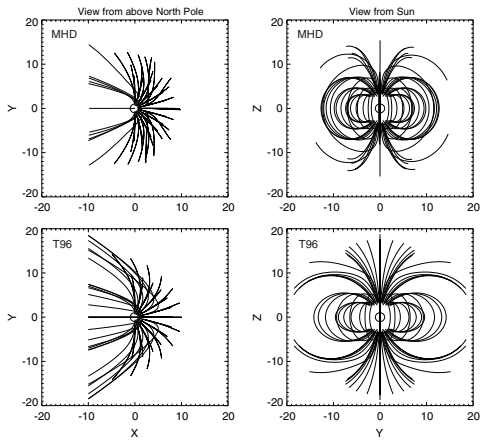


Fig. 11. Magnetic field lines drawn from the same starting points for the MHD model (top) and the T96 model (bottom) for northward IMF [Fenrich et al., 2001]. View from north pole is on the left and view from the Sun is on the right.

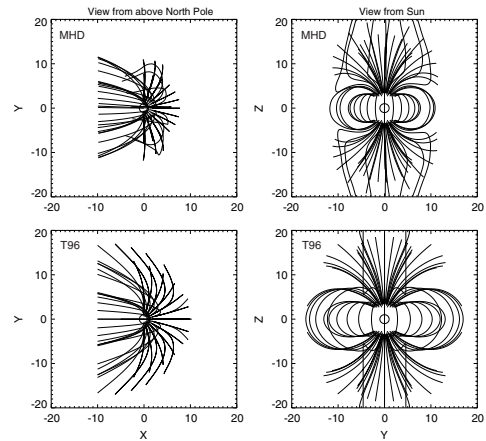


Fig. 12. Magnetic field lines drawn from the same starting points for the MHD model (top) and the T96 model (bottom) for southward IMF [Fenrich et al., 2001]. View from north pole is on the left and view from the Sun is on the right.

We expect the best agreement between the two models for northward IMF because the forces should be dominated by the normal stresses exerted by the solar wind plasma. Figure 11 shows field line tracings under northward IMF conditions for both models beginning both sets of tracings at the same locations in the magnetosphere. As can be seen in the lefthand pair of figures (the view from above the magnetosphere) the T96 field lines are more swept back than the MHD fields. Further the field lines end up in much different locations in the tail. In the right-hand pair we see a much different width of the terminator magnetosphere.

Figure 12 shows the corresponding diagrams for southward IMF. Now the tangential stresses imposed by reconnection come into play. Some of the MHD field lines are very much swept back as seen on the lefthand top panel. The changes in the T96 model from the northward case as seen in the lower left panel are more subtle. As before the field lines end up in much different locations in the tail. The righthand panels show an additional difference in the models, where interconnection occurs. In the MHD model reconnected field lines are carried by the flow. In the T96 model they are distributed in an ad hoc manner.

The strength of the field depression in each of the models for northward IMF is shown in Figure 13. The dashed line is a schematic trajectory of the Polar spacecraft and the righthand panel shows the time series along that trajectory. This righthand panel emphasizes that the MHD model produces a deeper cusp depression of the field than does the T96 model. However, only the T96 model has a reasonable ring current.

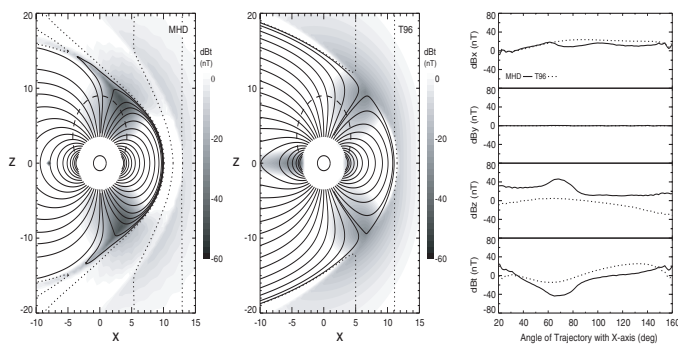


Fig. 13. Magnetic field magnitudes relative to dipole field in the MHD model (left), the T96 model (center) and along sample Polar trajectory (right) [Fenrich et al., 2001]. Shading indicates relative magnetic field depression.

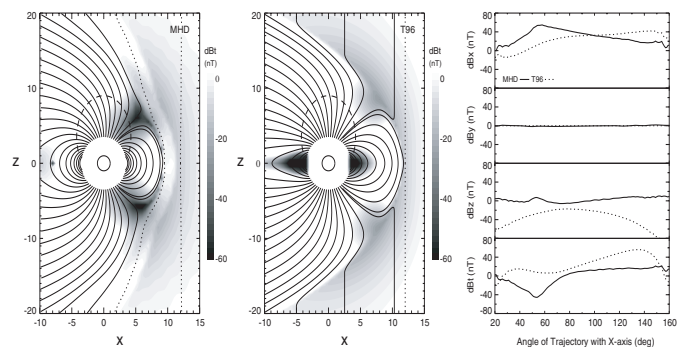


Fig. 14. Magnetic field magnitude relative to dipole field in the MHD model (left), the T96 model (center) and along sample Polar trajectory (right) for southward IMF [Fenrich et al., 2001]. Shading indicates relative field depression.

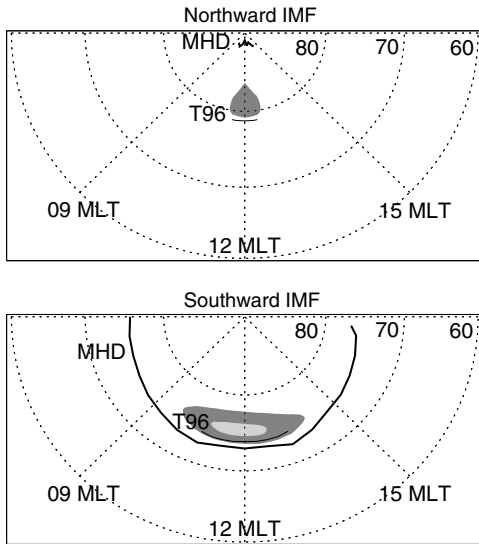


Fig. 15. Open closed boundaries for MHD and T96 models and MHD cusp position for northward IMF (top) and southward IMF (bottom) [Fenrich et al., 2001].

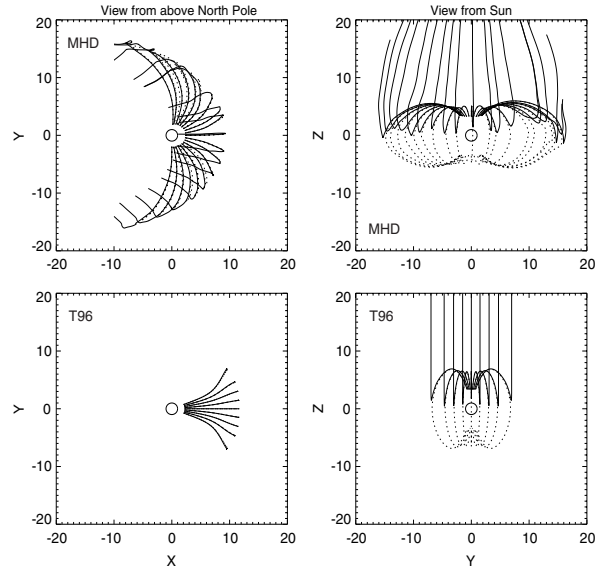


Fig. 16. First open magnetic field lines in the MHD and T96 models for southward IMF fields [Fenrich et al., 2001]. Left-hand panels show the view from the north pole and the right-hand panels show the view from the Sun.

When the IMF turns southward there are changes in both models as illustrated in Figure 14. In the MHD model the tail current moves inward and the cusp moves equatorward. In the T96 model the ring current strengths and the cusp depression (along the Polar orbit) weakens. This latter behavior is unexpected.

The last topic we examine is the boundary between the open and closed field lines. In Figure 15 we show these boundaries for northward and southward IMF for the two models together with the region of cusp associated depression for the MHD model. When the IMF is northward the MHD open-closed boundary is a small region near the pole, with the cusp near noon at about 82° latitude. The T96 open closed boundary lies equatorward of this cusp. When the IMF turns southward, the cusp broadens in the MHD model and the open-closed boundary moves equatorward of the cusp and spreads around the polar cap. The T96 open-closed boundary moves equatorward about 5° and approximately doubles its width in local time. Figure 16 shows the projected field line traces for the MHD and T96 models for southward IMF to emphasize this difference. In the T96 model the open closed boundary is narrowly confined.

SUMMARY AND CONCLUSIONS

The high latitude magnetosphere is very sensitive to the direction of the IMF. The cusp plasma is found poleward of the bifurcation line for southward IMF and equatorward of it for northward IMF. The MHD models correctly replicate this behavior. When the IMF is northward a thin current sheet forms in the magnetosphere at high latitudes and altitudes across which the magnetospheric magnetic field sharply reverses. In some senses this current layer is analogous to the subsolar magnetopause current layer for southward IMF but there is another current layer further out across which the field switches to the direction of the draped magnetosheath field. This layer separates field lines attached to the magnetosphere from those that are not.

The cusp is observed poleward of where it is expected from the T96 model. Further the T96 model does not predict accurately the depression in the magnetic field seen in the neighborhood of the cusp. The accuracy of the predicted pressure of the cusp plasma from the solar wind dynamic pressure gives some confidence in the knowledge of the average shape of the noon-midnight meridian magnetopause. The T96 model does not change as significantly from southward to northward IMF as we believe it should do. This is true for the field line configuration as well as the open-closed field-line boundary. Most importantly the field lines in the T96 and the MHD models go to quite different regions of the tail.

In short, the regular availability of magnetic field measurements from the Polar spacecraft has enabled us to refine our understanding of the configuration of the magnetic field in this important region of the magnetosphere. These measurements further will enable future generations of empirical models to provide more accurate magnetic predictions. While MHD models provide some advantages over empirical models they too are only approximations and especially for northward IMF cannot resolve the thin currents often found near the cusp.

ACKNOWLEDGMENTS

This research was supported by the National Aeronautics and Space Administration under research grant NAG5-7721.

REFERENCES

- Fedder, J. A., S. P. Slinker et al.. A first comparison of POLAR magnetic field measurements and magnetohydrodynamic simulation results for field-aligned currents, *Geophys. Res. Lett.*, **24**, 2491-2494 (1997).
- Fenrich, F. R., J. G. Luhmann, J. A. Fedder, S. P. Slinker and C. T. Russell, A global MHD model and empirical magnetic field model investigation of the magnetospheric cusp, *J. Geophys. Res.*, submitted, (2001).
- Fuselier, S. M., K. H. Trattner et al. Cusp observations of high and low-latitude reconnection for northward IMF, *J. Geophys. Res.*, **105**, 253-266, (2000).
- Petrinec, S. M. and C. T. Russell, An empirical model of the size and shape of the near-Earth magnetotail, *Geophys. Res. Lett.*, **20**, 2695-2698 (1993a).
- Petrinec, S. M. and C. T. Russell, External and internal influences on the size of the dayside terrestrial magnetosphere, *Geophys. Res. Lett.*, **20**(5): 339-342 (1993b).
- Petrinec, S. M. and C. T. Russell, Hydrodynamic and MHD equations across the bow shock and along the surfaces of planetary obstacles, *Space Sci. Rev.*, **79**, 757-791 (1997).
- Roelof, E. C. and D. G. Sibeck, Magnetopause shape as a bivariate function of interplanetary magnetic field B_z and solar wind dynamic pressure, *J. Geophys. Res.*, **98**, 21,421-21,450 (1993).
- Russell, C. T., J. A. Fedder et al., Entry of Polar spacecraft into the polar cusp under northward IMF conditions, *Geophys. Res. Lett.*, **25**, 3015-3018 (1998).
- Russell, C. T., G. Le et al., Cusp observations of high- and low-latitude reconnection for northward IMF: An alternate view, *J. Geophys. Res.*, **105**, 5489-5495 (2000).
- Russell, C. T. and R. L. McPherron, The magnetotail and substorms, *Space Sci. Rev.*, **15**, 205-266, (1973).
- Savin, S. P., S. A. Romanov et al., The cusp/magnetosheath interface on May 29, 1996: Interball-1 and Polar observations, *Geophys. Res. Lett.*, **25**, 2963-2966 (1998).
- Scudder, J. D., F. S. Mozer et al. Fingerprints of reconnection, *J. Geophys. Res.*, to be submitted, (2001).
- Shue, J. H., P. Song, C. T. Russell, M. F. Thomsen and S. M. Petrinec, Dependence of magnetopause erosion on southward IMF, *J. Geophys. Res.*, submitted, (2001).
- Tsyganenko, N. A., A solution of the Chapman-Ferraro problem for an ellipsoidal magnetopause, *Planet. Space Sci.*, **37**(9), 1037-1046 (1989).
- Tsyganenko, N. A., Effects of the solar wind conditions on the global magnetospheric configuration as deduced from data-based field models, in *Proceedings of the ICS-3 Conference on Substorms*, Versailles, France, ESA, (1996).
- Tsyganenko, N. A. and C. T. Russell, Magnetic signatures of the distant polar cusps: Observations by Polar and quantitative modeling, *J. Geophys. Res.*, **104**, 24,939-24,955 (1999).
- Zhou, X.-W. and C. T. Russell, The location of the high latitude polar cusp and the shape of the surrounding magnetopause, *J. Geophys. Res.*, **102**, 105-110 (1997).
- Zhou, X.-W., C. T. Russell et al., The polar cusp location and its dependence on dipole tilt, *Geophys. Res. Lett.*, **26**, 429-432 (1999).
- Zhou, X.-W., C. T. Russell et al., Solar wind control of the polar cusp at high altitudes, *J. Geophys. Res.*, **105**, 245-251 (2000).
- Zhou, X. W., C. T. Russell, G. Le, S. A. Fuselier and J. D. Scudder, The factors controlling the diamagnetic pressure in the polar cusp, *Geophys. Res., Lett.*, in press, (2001).